

RESEARCH ARTICLE

Diffusion profiles in *L. lactis* biofilms under different conditions

Jonas Chodorski¹ | Jan Hauth² | Dorina Strieth¹ | Andreas Wirsén² | Roland Ulber¹ 

¹ Institute of Bioprocess Engineering, Department of Mechanical and Process Engineering, TU Kaiserslautern, Kaiserslautern, Germany

² Fraunhofer ITWM, Kaiserslautern, Germany

Correspondence

Prof. Dr. Roland Ulber, Institute of Bioprocess Engineering, TU Kaiserslautern, Gottlieb-Daimler-Str. 49, 67663 Kaiserslautern, Germany.

Email: ulber@mv.uni-kl.de

Funding information

Deutsche Forschungsgemeinschaft, Grant/Award Numbers: LA 1454/6-1, SFB 926 - ID 172116086, UL 170/14-1

Abstract

Despite being an important topic in biofilm research, we still know little about diffusion in biofilms. Emerging biofilms of *Lactococcus lactis* growing in custom-made flow-cells were monitored and diffusion constants across the height of the biofilms recorded. The biofilms showed different diffusional behavior with regard to flow rate and pH variations, despite growing to similar thickness. At a higher flow rate, the biofilm exhibits slower diffusion compared to the reference cultivation at lower flow rate. By increasing pH, the biofilm exhibited fast growth and little difference in diffusion compared to the reference cultivation. Furthermore, the diffusion inside of the biofilms differed depending on the position in the flow-cell. The present study reveals new insights in how external factors can affect structure and density of biofilms. The method can be reliably used for *L. lactis* biofilms with a thickness up to 120 μm .

KEYWORDS

biofilm, diffusion, flow-cell, FRAP, *Lactococcus lactis*

1 | INTRODUCTION

According to a generally accepted definition, biofilms are microbial communities adhered to each other and/or surfaces or boundary layers [1]. Cells attach to surfaces with growing colonies embedding themselves in extracellular polymeric substances (EPS), which mainly consist of water, polysaccharides, lipids, proteins, extracellular DNA and lysis products. This results in a complex matrix whose composition has not yet been fully elucidated [2]. EPS function as protective layer against biotic and abiotic con-

ditions such as temperature fluctuation, drought, or even antibiotics. Biofilm formers adhere naturally to surfaces and no chemicals harmful to humans need to be used for immobilisation [3]. Thus, in industrial applications, biofilms can be advantageous, as their self-immobilizing nature can be employed for simplifying downstream processing and make biotechnological processes easier and more efficient [4]. Product purification of secreted substances is facilitated by immobilized cells and higher productivity can be achieved in continuous processes [5], as the growth rate can be decoupled from the dilution rate. A mature biofilm can consist not only of dense cell clusters in an extracellular matrix, but it can also contain voids, grooves and channels [6,7]. However, mass transport processes in biofilms have still not yet been fully explored.

Abbreviations: EPS, extracellular polymeric substances; FRAP, fluorescence recovery after photobleaching; MRS, de Man, Rogosa, Sharpe medium

This is an open access article under the terms of the [Creative Commons Attribution-NonCommercial-NoDerivs](https://creativecommons.org/licenses/by-nc-nd/4.0/) License, which permits use and distribution in any medium, provided the original work is properly cited, the use is non-commercial and no modifications or adaptations are made.

© 2020 The Authors. *Engineering in Life Sciences* published by Wiley-VCH GmbH

According to the current state of knowledge, channels (as in *Bacillus subtilis* [8]) for directed mass transport are available only in very rare cases. In most cases, distribution is by diffusion, which is driven by concentration gradients in the biofilm [9] and between the bulk phase and the biofilm. This results in spatially distributed heterogeneous cultivation conditions, in which cells in the most different growth stages can be found. Therefore, it is important to get an idea of how diffusion in biofilms of a given species works in order to better assess cultivation conditions; thus, saving time on trial-and-error approaches.

The main focus of biofilm diffusion research used to be on transport on the surface, i.e. from bulk fluid into the biofilm or out of it; often gas transport was investigated [10–13]. There have also been several studies trying to simulate the diffusion and other transport processes inside of or into biofilms [14–19]. Current publications are mainly dealing with multispecies and pathological biofilms (e.g. [20–22]). Diffusional measurements in biofilms were traditionally carried out via sensors and electrodes [23–25], which disturbs and damages the biofilm. In contrast, a non-invasive method for assessing diffusion in biofilms is fluorescence recovery after photobleaching (FRAP), where a short, but strong laser pulse bleaches a region of interest and the recovery time of fluorescence is measured, from which then diffusional constants can be calculated. Since the 70s, several diffusion models have been developed [26,27], with the latest model employing Markov-Chain Monte Carlo methods to reduce common artefacts found in FRAP measurements [28]. With this model, it is possible to calculate diffusional constants more exactly from FRAP measurements.

In this study, the influence of different cultivation conditions on diffusion of a dextran conjugated fluorescein-isothiocyanat (FITC) in an axenic biofilm using nisin producing *Lactococcus lactis* (DSM 20729) as biofilm former was investigated using FRAP. Cultivations were conducted in a custom-made flow cell [29] using a two-step procedure in which at first (i) biofilm adhesion was achieved in a batch system followed by (ii) a 12 h continuous cultivation during which the influence of pH and volume flow on diffusion inside the biofilm were investigated.

2 | MATERIALS AND METHODS

2.1 | Pre-culture

Biofilms of *Lactococcus lactis* (DSM 20729) were anaerobically cultivated in a flow-cell system described by Schlegel [29], with an optimized dye inlet and chamber [28]. Pre-culture was carried out in a 100 mL bottle at 30°C in 100 mL

PRACTICAL APPLICATION

Biofilms, while being the main mode of growth for microorganisms on earth, have not yet been thoroughly understood. An important step towards better understanding is elucidating the diffusional processes inside the biofilm. The approach described in this paper can be of use in this endeavour. By combining a novel model for assessment of diffusion constants with confocal FRAP microscopy, it is possible to generate diffusion profiles of biofilms that can help researchers better understand the biofilms they are working with and thus enabling them for example to optimize their process conditions.

MRS (de Man, Rogosa, Sharpe) medium [30] at a pH of 7 with 20 g·L⁻¹ glucose inoculated from the same cryo batch for all experiments. The headspace was flushed with nitrogen to ensure an anaerobic atmosphere. The bottle was shaken at 130 rpm until an OD₆₀₀ of 4 was reached, which was used to inoculate batch culture to a starting OD₆₀₀ of 0.2.

2.2 | Experimental set-up

As described above, the two-step cultivation started with the inoculation phase as batch process. The batch process allows the bacteria to initially attach to the surface to form a biofilm. Therefore, 100 mL of MRS medium (pH 7, 20 g·L⁻¹ glucose) with an initial OD₆₀₀ of 0.2 were pumped (Ismatec IPC peristaltic pump, IDEX Health & Science, Wertheim, Germany) through the flow cell for 16 h with a volume flow of 5 mL·min⁻¹. Breaks of 60 min after 15 min pumping the cell suspension facilitated bacterial adhesion. After 16 h batch cultivation was switched to a continuous process using MRS medium with 10 g·L⁻¹ glucose for 12 h. The influence of different pH values (pH 7 and 5.5) of the medium and different flow rates (0.25 mL·min⁻¹ and 0.5 mL·min⁻¹) were investigated (n = 5). The experiments were carried out during anaerobic continuous culture under the microscope and were not moved during cultivation. The microscope stage was covered with a hood that allowed for a constant temperature of 30°C during the continuous cultivation. At the end of each cultivation, final biofilm thickness was non-invasively determined via spectral domain Optical Coherence Tomography (sdOCT).

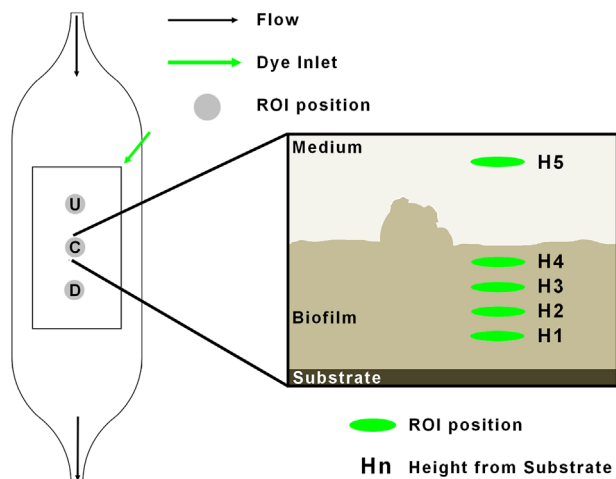


FIGURE 1 Flow cell setup. Three evenly-spaced positions on the 10×20 mm sample were chosen: upstream (U), center (C); downstream (D). Dye was applied from the upstream corner of the sample. At each position, five different heights were measured: From the substrate $50 \mu\text{m}$ (H1), $100 \mu\text{m}$ (H2), $150 \mu\text{m}$ (H3), $200 \mu\text{m}$ (H4), $700 \mu\text{m}$ (H5, water control)

2.3 | FRAP data acquisition

FRAP measurements were carried out on a Leica SP5 II confocal laser scanning microscope (Leica Microsystems, Wetzlar, Germany) with an active beam expander module. Measurement was taken after 5, 7, 8, 9, 10, 11 and 12 h of continuous cultivation (t_5 to t_{12}). At each time point $100 \mu\text{L}$ FITC Dextran 4 kDa (FD4) (TdB Consultancy AB, Uppsala, Sweden) at a concentration of $225 \text{ mg}\cdot\text{mL}^{-1}$ resulting in a final concentration of $15 \text{ mg}\cdot\text{mL}^{-1}$ were added to the flow chamber via a separate inlet. This fluorescence dye was used since it has no known biological influence on prokaryotes [31]. For an optimal spread of the fluorescence dye a constant volume flow for 2 min was ensured. During FRAP measurements the volume flow was stopped to not disturb recordings. FRAP time series were taken with a 63×0.9 water immersion objective (Leica Microsystems, Wetzlar, Germany) in the biofilm at distances of 50, 100, 150, 200 and $700 \mu\text{m}$ (bulk fluid, “water control”) from the sample surface (H1 to H5, Figure 1). The parameters were as follows: 256 px image size, 1400 Hz scanning speed (bidirectional), 6x zoom, $20 \mu\text{m}$ circular bleach radius—the best compromise between image acquisition time and measurable area—75% laser power (Argon laser), 5% AOTF (Acusto-Optical Tunable Filter) (scan)/100% AOTF (bleach), pinhole 2 AU (Airy Units). Each measurement was separated into a pre-bleach (15 frames), bleach (five frames) and post-bleach (60 frames) phase. Frame time was set to 0.195 s and 8-bit TIFF (Tagged Image File Format) was used as data format. Three positions for measurement were chosen evenly spaced on the

10×20 mm sample; thus, essentially dividing the sample in three compartments—upstream (U), center (C), downstream (D) (Figure 1).

2.3.1 | Data processing

FRAP data were processed and diffusion constants were calculated according to the improved FRAP model by Hauth et al. [28]. From the diffusional constants the adjusted diffusion

$$D_a = D_B/D_W \quad (1)$$

could be calculated., with D_B being the diffusion constant in the biofilm and D_W being the diffusion constant in the medium (= water control). This allows assessing how diffusively dense the biofilm is compared to the medium. With this, a heatmap for each growth condition and each position on the sample was generated using the free software R [32] with the heatmap.2 function.

3 | RESULTS AND DISCUSSION

3.1 | Biofilm formation

After ensuring identical conditions during batch mode in all experiments, differences in growth during continuous mode were already macroscopically apparent. Under regular conditions (pH 5.5 and flow rate of $0.25 \text{ mL}\cdot\text{min}^{-1}$), full biofilm opacity, i.e. no surface structures being visible under the biofilm, occurred between 6 and 8 h. By doubling the flow rate ($0.5 \text{ mL}\cdot\text{min}^{-1}$) full biofilm opacity was achieved after 5 h. The change of pH 5.5 to 7 resulted in a faster height growth and full coverage of the surface was reached after 3 h in continuous mode. For all conditions, final biofilm thickness after 12 h of cultivation was between $221 \pm 41 \mu\text{m}$ with mushrooms up to $367 \mu\text{m} \pm 39 \mu\text{m}$ (Figure 2), which is significantly higher than other reported biofilm thicknesses for *L. lactis* (e.g. [33]: $50\text{--}100 \mu\text{m}$ after 15 h in a microtiter plate). However, the biofilm cultivated at pH 7 reached the final thickness 2 h earlier. The biofilm under pH 7 conditions after 10 h of cultivation grew as high as $406 \mu\text{m}$ and made reliable FRAP measurements difficult since the laser was not able to properly penetrate the biofilm anymore.

3.2 | FRAP measurements

In order to compare the diffusion rates between different cultivation conditions, the D_B/D_W ratio was calculated as

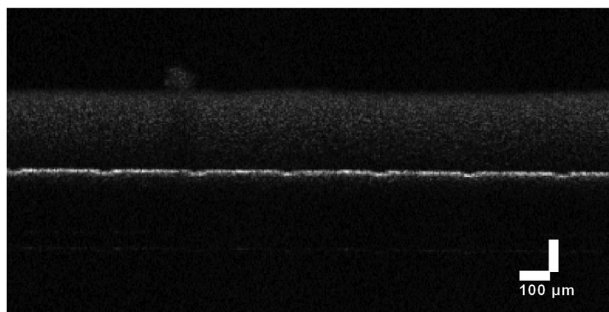


FIGURE 2 Biofilm after 10 h of cultivation with pH7 (exemplary segment from full biofilm). Height of mushroom structure is $328 \mu\text{m}$, height of bulk biofilm is $251 \mu\text{m}$. Taken with Thorlabs Ganymede II (Thorlabs GmbH, Lübeck, Germany)

D_a and presented in the form of heatmaps (Figure 3). Since the dye employed is considered biologically inert with a net charge of 0 [25], effects of the extracellular matrix originating from DNA or polysaccharides or other compounds on its diffusion can be disregarded. In all experiments, only the values for the heights 100, 150 and $200 \mu\text{m}$ could be considered, as it became apparent that at height $50 \mu\text{m}$ light diffraction from the biofilm layers above prevented proper measurements.

Under reference conditions (Figure 3(1)), the Position Upstream (Pos U) and Center (Pos C) behave similarly, with both positions exhibiting low D_a in the lowest stratum while the upper strata show a generally higher D_a . Position Downstream (Pos D) deviates from this strongly at 9 h, where D_a is strongly decreased, after which it increases again in the upper strata, while staying low in the lower stratum. This is in accordance with the findings of Yang et al. [23], where local mass transfer coefficients were shown to decrease with increasing distance from the boundary layer and how it can vary horizontally and vertically. They concluded that the influence of hydrodynamics decreases towards the bottom of the biofilm and described “unexplained variabilities,” which they attributed to the heterogeneity of the biofilm. In the early phase of growth, the higher D_a values in the upper strata can be attributed to two factors: (a) the biofilm not having grown either to the respective height at that position, or (b) an overall very high water content in the emerging biofilm, as the biofilm in this experiment is fully hydrated and undisturbed. As mentioned earlier, other studies used invasive methods to analyse diffusion. Hou et al. showed for *Streptococcus mutans* biofilms a decreased bacterial density with an increased sucrose concentration [34], so conversely, at this position it might be possible that due to lower carbon

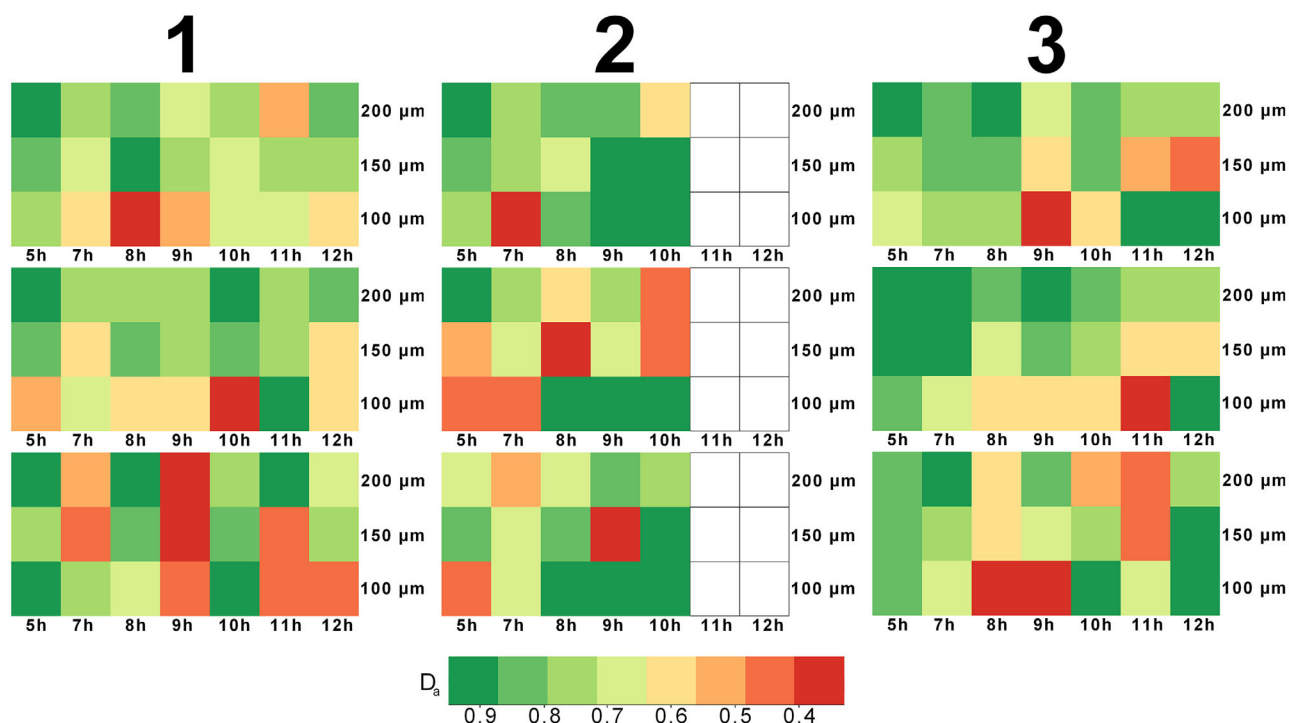


FIGURE 3 D_a , as ratio of D_b/D_w plotted over time and height. From top to bottom according to the positions on the sample (flow cell, left side) – position U (upstream), position C (center), position D (downstream). (1) Reference cultivation at pH 5.5 and $0.25 \text{ mL}\cdot\text{min}^{-1}$ flow rate, (2) cultivation at pH 7 and $0.25 \text{ mL}\cdot\text{min}^{-1}$; for the sake of completeness the grid is displayed for up to 12 h, (3) cultivation at pH 5.5 and $0.5 \text{ mL}\cdot\text{min}^{-1}$ flow rate. Green colour indicates faster diffusion, red colour indicates slower diffusion compared to water

availability the cell density is actually higher than at the upstream positions.

Since FITC fluorescence is best observed in pH conditions above 5 [35], pH variance into neutral/basic was tested. pH itself should not have a significant influence on diffusion in the biofilm [25], but on growth of the biofilm. At pH 7 (Figure 3(2)), D_a is approaching the water value over the whole cultivation time at Pos U. After that a much higher D_a could be detected in the lower strata, although Pos C and Pos D both showed an overall lower diffusion at the beginning, with a switch to high D_a towards the end of the cultivation. Adamberg et al. [36] showed that certain lactic acid bacteria, among them *L. lactis* subsp. *lactis*, exhibit a higher growth rate at pH values over 6, explaining the earlier reached high thickness of the biofilm during cultivation. However, it is also known that in the same way a higher pH facilitates growth rate, it hinders product formation, which is a concern in productive biofilms such as the *L. lactis* strain used in this study [37,38], as a balance must be struck between biomass growth and productivity. In general, the data for this experiment is, compared to the reference, less conclusive and with progressing cultivation time, standard deviations increased. The more biomass above the measured layer, the less light penetration—and thus, a worse signal/noise ratio, leading to higher standard deviation. This effect could be alleviated by using a dye that has higher extinction/emission maxima, but to date there is no dye available in higher wavelength ranges that would be suitable for FRAP experiments. Considering the spatial resolution of the generated profiles, it is important to keep in mind that the ROI for these measurements is only 20 μm ; thus, they should only be considered “snapshots” of specific spots of the total biofilm. However, due to the experimental setup, it was not possible to measure more spots and heights. A reason is that for the diffusion measurement, keeping a steady flow throughout the whole process would warp results. However, in order for the biofilm to grow, flow cannot be turned off for a prolonged time, which would be the result of having more positions and heights—thus a compromise must be made. In this case separating the biofilm in three distinct and representative sections (upstream, center, downstream).

By doubling the flow rate, a dilution rate of $20 \cdot \text{h}^{-1}$ was achieved. Here, D_a was close to 1 among all positions at the top layer at the early timepoints (Figure 3(3)), with a slight decrease towards the end of cultivation. However, at Pos D the diffusion in the upper strata decreased more compared to Pos U and C, with e.g. 150 μm at t11 with a D_a of 0.44 ± 0.03 . D_a decreased over time in the lower strata at Pos U and Pos C with very low values during the cultivation mid-point around 9 h. The same phenomenon was already observed under reference conditions, with both showing low D_a in the bottom stratum at the mid-point (upstream,

downstream) or from mid-point onwards (center), suggesting that pH has a higher impact on diffusion in biofilms than flow rate. Ohl described that biofilms cultivated at higher flow rates, are more prone to form channels and voids [39]. Other studies suggest that higher flow rates led to higher cell densities to alleviate the higher shear stress [40,7]. Liu et al. found an increase in EPS to biomass ratio under higher flow velocities [41] which leads to a higher water content and thus faster diffusion. Regarding the literature a combination of increased amount of channels and EPS content of the biofilm paired with higher cell densities led to the same diffusion measured in the reference experiment. However, it must be considered that multiple species of biofilm formers have been used in the cited literature. This means that the threshold for the amount of shear stress leading to increased cell density or EPS can be organism specific.

All experiments have in common that the upstream positions (Pos U and Pos C) behaved similarly and that Position D deviates most. In addition, all experiments showed around the cultivation mid-point the lowest diffusion (at around 9 h, for pH7 at 7 h) in the measured strata. Seker et al. showed that after a biofilm has reached a certain critical thickness the diffusion is limited to the lower layers and the biofilm thickness decreases again to facilitate diffusion [42]. Here, no decrease in biofilm could be observed; however, it is possible that there is still diffusional limitation present in the lower strata, leading to the formation of channels to increase diffusion again. In the upper strata, diffusion was expectedly faster, as either the biofilm hadn't grown to the respective height yet or because certain effects like osmotic pressure of extracellular substances increase water content in the upper layers and thus increasing diffusional speed [43]. General reasons for a change in diffusional speed are manifold. The cell density itself plays an important role as there are areas with higher and lower cell density and very small molecules are virtually unphased considering changes in diffusional speed [6]. Further factors to consider for diffusion measurements—as those always entail the sum of possible molecular movements—are for example the tortuosity, as discussed in e.g. [44]. Here, actual “obstacles decrease motion speed compared to unconstrained free space” [45], i.e. due to higher cell density the molecules simply take longer to circumnavigate those obstacles. The presence of channels and voids would also lead to a diffusion constant close or equal to that of water, but there are conflicting results considering the existence, the exact conditions for formation of those channels and an increase/decrease in cell density. The mean or overall biofilm diffusion ratio, i.e. the mean of all D_a of all heights and all times for the reference cultivation of 0.85 is slightly higher than the ratio given by Stewart [10] of 0.81, but it

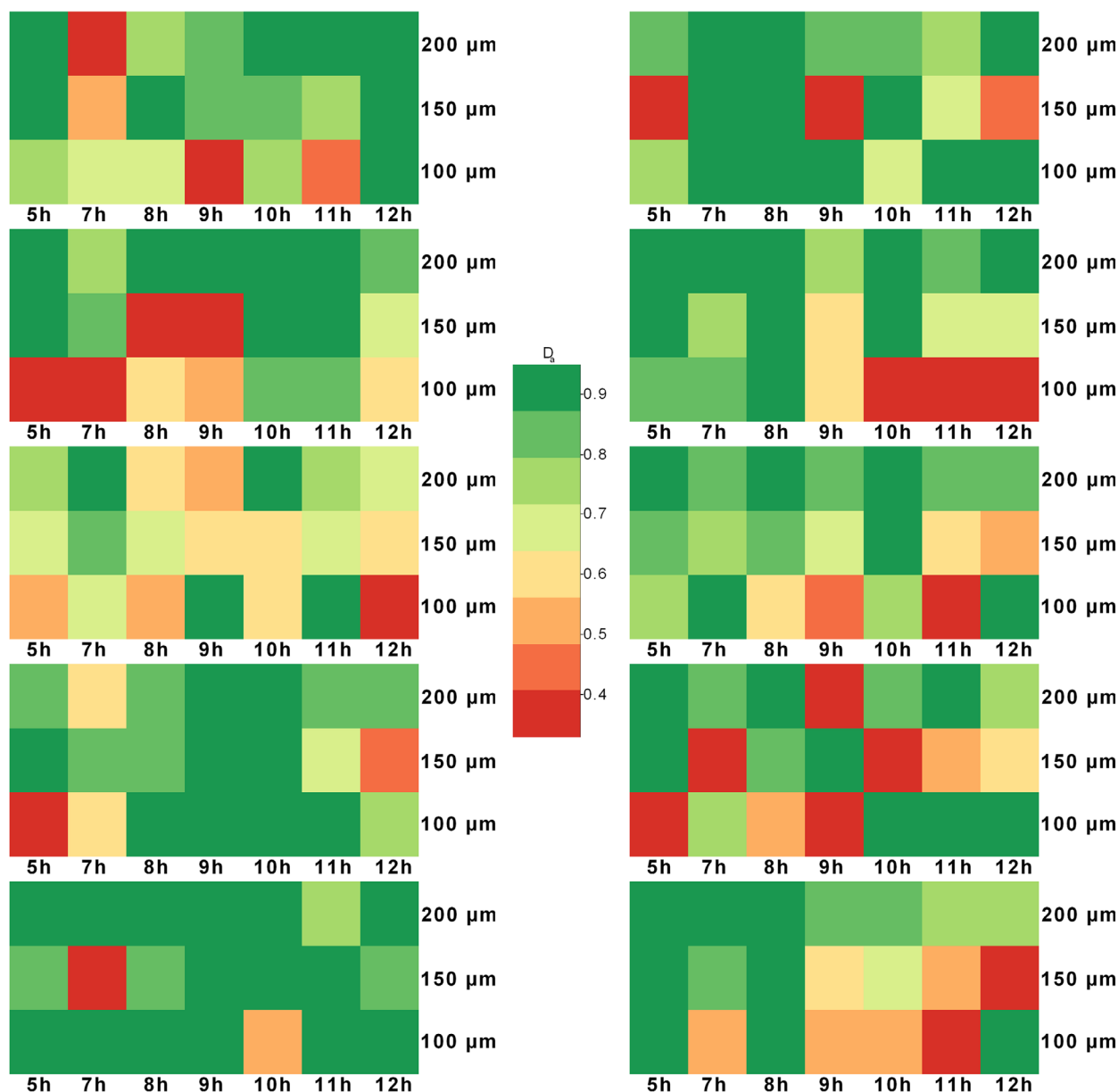


FIGURE 4 Plots for all measurements at position U for reference cultivation (left, $0.25 \text{ mL}\cdot\text{min}^{-1}$, pH 5.5) and double flow cultivation (right, $0.5 \text{ mL}\cdot\text{min}^{-1}$, pH 5.5)

must be considered that in this study a fully hydrated, living and growing biofilm was observed, as opposed to other experiments with comparably dry, i.e. not fully hydrated biofilms.

3.3 | Variation in biofilm growth

A big challenge working with biofilms is the heterogeneity of the biofilms resulting in high standard deviations of biological replicates (e.g. [46]). In this work, sometimes standard deviations of measured diffusion increased with increasing biofilm thickness. To get a better insight into

the raw data, single plots for each biological replicate, exemplarily for Position U for reference cultivation and double flow cultivation are given (see Figure 4). For emphasis, outliers were not removed. On the left side, the reference shows widely differing behaviour, as evident in the difference between the two bottom experiments and the second and third experiment. Here, lower strata show a slower diffusion throughout, whereas experiments 4 and 5 behave conversely with very fast measured diffusion even in the lower strata. On the right side, experiment 1 exhibits noticeable deviation, whereas experiments 2–4 have in common decreasing D_a values in the lower strata over time. Here, it becomes obvious that biofilms,

despite keeping all outside conditions as constant as possible, still can behave very differently from experiment to experiment (see also [46]). Due to the setup and timeframes, parallel cultivation and measurement was not possible, as well as carrying out all experiments from a single propagated pre-culture. Since the experimental setup allowed for reliable and reproducible measurements of the biofilms—as evidenced by the tight variance in the medium control (6.2% standard deviation between experiments for reference condition)—the observed high variance must originate in the biofilms themselves. As stated by de Beer et al. [47], complexity, i.e. heterogeneity, of *Klebsiella* and *Pseudomonas* biofilms, can increase with increasing flow velocity, although in this study the cultivation with the highest flow rate showed the least variance between experiments compared to the other cultivations. With biofilms possessing, as mentioned earlier, channels and voids, but also clusters of higher cell density whose distribution is always unique to each biofilm—and thus creating the possibility of a local sterically unfavourable spot, as e.g. discussed by [46]—it is clear that the issues at hand are caused by a lack of data.

4 | CONCLUSION

The goal of this study was to employ a recently developed model for assessing diffusion constants via the FRAP method to generate diffusion profiles for undisturbed, growing biofilms of *L. lactis* under different cultivation conditions. Diffusion profiles were generated in the form of heatmaps, where the adjusted diffusion D_a was used to compare diffusion in different layers of the growing biofilm. Despite the biofilms reaching similar final heights under different conditions, diffusion profiles differed between conditions, as well as between different positions for each condition. However, the downstream position showed the highest similarity between all conditions and there was a distinct drop of D_a at cultivation mid-point of unknown origin. Here, it would be indicated to conduct gene expression analysis in order to elucidate if there are any major changes in gene expression at that point. Issues still present include low data volume dictated by the experimental setup, the elusive influence of EPS on diffusion and the inherent heterogeneity of biofilms. Comparison of replicate experiments showed that despite the method having adequate accuracy and reproducibility, biofilms can still grow in a different fashion from experiment to experiment, making general assumptions about diffusional behaviour of biofilms difficult and posing a challenge to researchers. It was demonstrated that a diffusion profile of a living, growing and undisturbed biofilm inside of a flow cell can be generated.

ACKNOWLEDGMENTS

RU and AW designed the research. JC conducted experiments. JC and DS wrote the article. JH processed the FRAP data. This work was funded by the Deutsche Forschungsgemeinschaft (German Research Foundation) under grants LA 1454/6-1, UL 170/14-1 and Project-ID 172116086 – SFB 926.

Open access funding enabled and organized by Projekt DEAL.

CONFLICT OF INTEREST

The authors have declared no conflict of interest.

DATA AVAILABILITY STATEMENT

The data that support the findings of this study are available from the corresponding author upon reasonable request.

ORCID

Roland Ulber  <https://orcid.org/0000-0002-7674-0967>

REFERENCES

1. Costerton, J. W., Lewandowski, Z., Caldwell, D. E., Korber, D. R., et al., Microbial Biofilms. *Annu. Rev. Microbiol.* 1995, 49, 711–745.
2. Flemming, H. - C., Neu, T. R., Wozniak, D. J., The EPS Matrix: The “House of Biofilm Cells”. *J. Bacteriol.* 2007, 189, 7945–7947.
3. Garrett, T. R., Bhakoo, M., Zhang, Z., Bacterial adhesion and biofilms on surfaces. *Prog. Nat. Sci.* 2008, 18, 1049–105.
4. Muffler, K., Lakatos, M., Schlegel, C., Strieth, D., et al., Application of Biofilm Reactors in White Biotechnology. *Adv. Biochem. Eng. Biotechnol.* 2015, 146, 123–161.
5. Chaudry, S., Bahri, P., Moheimani, N., Potential of Milking of Microalgae Grown on Biofilm Photobioreactor for Renewable Hydrocarbon Production. 2017. <https://doi.org/10.1016/B978-0-444-63965-3.50418-9>.
6. de Beer, D., Stoodley, P., Lewandowski, Z., Measurement of Local Diffusion Coefficients in Biofilms by Microinjection and Confocal Microscopy. *Biotechnol. & Bioeng.* 1997, 53, 151–158.
7. Stoodley, P., Lewandowski, Z., Boyle, J. D., Lappin-Scott, H. M., Structural Deformation of Bacterial Biofilms Caused by Short-Term Fluctuations in Fluid Shear: An In Situ Investigation of Biofilm Rheology. *Biotechnol. & Bioeng.* 1999, 65, 83–92.
8. Wilking, J. N., Zaborzaev, V., de Volder, M., Losick, R., et al., Liquid transport facilitated by channels in *Bacillus subtilis* biofilms. *PNAS* 2013, 110, 848–852.
9. Stewart, P. S., Diffusion in Biofilms. *J. Bacteriol.* 2003, 185, 1485–1491.
10. Stewart, P. S., Theoretical aspects of antibiotic diffusion into microbial biofilms. *Antimicrob. Agents Chemother.* 1996, 40, 2517–2522.
11. Picioreanu, C., van Loosdrecht, M. C. M., Heijnen, J. J., A theoretical study on the effect of surface roughness on mass transport and transformation in biofilms. *Biotechnol. & Bioeng.* 2000, 68, 355–369.
12. Wäsche, S., Horn, H., Hempel, D. C., Influence of growth conditions on biofilm development and mass transfer at the bulk/biofilm interface. *Water Research* 2002, 36, 4775–4784.

13. Rani, S. A., Pitts, B., Stewart, P. S., Rapid Diffusion of Fluorescent Tracers into Staphylococcus epidermidis Biofilms Visualized by Time Lapse Microscopy. *Antimicrob. Agents Chemother.* 2005, 49, 728–732.
14. Yabannavar, V. M., Wang, D. I. C., Analysis of Mass Transfer for Immobilized Cells in an Extractive Lactic Acid Fermentation. *Biotechnol. & Bioeng.* 1991, 37, 544–550.
15. Gonpot, P., Smith, R., Richter, A., Diffusion limited biofilm growth. *Modelling Simul. Mater. Sci. Eng.* 2000, 8, 707–726.
16. Horn, H., Hempel, D. C., Simulationsrechnungen zur Beschreibung von Biofilmsystemen, *CIT* 2000, 10, 1234–1237.
17. Horn, H., Wäsche, S., Hempel, D. C., Simulation of biofilm growth, substrate conversion and mass transfer under different hydrodynamic conditions. *Water Sci. & Technol.* 2002, 46, 249–252.
18. Olivera-Nappa, A., Picioareanu, C., Asenjo, J. A., Non-homogeneous Biofilm Modeling Applied to Bioleaching Processes. *Biotechnol. & Bioeng.* 2010, 106, 660–676.
19. Guélon, T., Mathias, J. D., Deffuant, G., Influence of the spatial structure on the effective nutrient diffusion in bacterial biofilm. *J. Biol. Phys.* 2012, 38, 573–588.
20. Süß, M., De Visscher, A., Effect of diffusion limitation and substrate inhibition on steady states of a biofilm reactor treating a single pollutant. *J. Air & Waste Man. Assoc.* 2019, 69, 1107–1115.
21. D'Acunto, B., Frunzo, L., Klapper, I., Mattei, M. R., et al., Mathematical modeling of dispersal phenomenon in biofilms. *Math. Biosci.* 2019, 307, 70–87.
22. Kosztołowicz Tadeusz, Metzler Ralf. Diffusion of antibiotics through a biofilm in the presence of diffusion and absorption barriers. *Physical Review E.* 2020, 102, 032408.
23. Yang, S., Lewandowski, Z., Measurement of Local Mass Transfer Coefficient in Biofilms. *Biotechnol. & Bioeng.* 1995, 48, 737–744.
24. Beuling, E. E., van den Heuvel, J. C., Ottengraf, S. P. P., Diffusion Coefficients of Metabolites in Active Biofilms. *Biotechnol. & Bioeng.* 2000, 67, 53–60.
25. Zhang, Z., Nadezhina, E., Wilkinson, K. J., Quantifying Diffusion in a Biofilm of *Streptococcus mutans*. *Antimicrob. Agents Chemother.* 2011, 55, 1075–1081.
26. Axelrod, D., Koppel, D. E., Schlessinger, J., Elson, E., et al., Mobility measurement by analysis of fluorescence photobleaching recovery kinetics. *J. Biophys.* 1976, 16, 1055–1069.
27. Soumpasis, D. M., Theoretical analysis of fluorescence photobleaching recovery experiments. *J. Biophys.* 1983, 41, 95–97.
28. Hauth, J., Chodorski, J., Wirsén, A., Ulber, R., Improved FRAP measurements on biofilms. *J. Biophys.* 2020, 118, 2354–2365.
29. Schlegel, C., Produktive Biofilme auf mikrostrukturierten Metalloberflächen. Dissertation 2016. Technical University Kaiserslautern.
30. de Man, J. D., Rogosa, M., Sharpe, M. E., A medium for the cultivation of lactobacilli. *J. Appl. Bact.* 1960, 23, 130–135.
31. Arbeitskreis "Human- und ökotoxikologische Bewertung von Markierungsmitteln in Gewässern", Human- und ökotoxikologische Bewertung von Markierungsmitteln in Gewässern. *Grundwasser* 1997, 2, 61–64.
32. R Core Team, R: *A Language and Environment for Statistical Computing*. R Foundation for Statistical Computing 2019, Vienna, Austria. <https://www.R-project.org/>.
33. Oxaran, V., Ledue-Clier, F., Dieye, Y., Herry, J. - M., et al., Pilus biogenesis in *Lactococcus lactis*: molecular characterization and role in aggregation and biofilm formation. *PLoS ONE* 2012, 7, e50989.
34. Hou, J., Wang, C., Rozenbaum, R. T., Gusnaniar, N., et al., Bacterial Density and Biofilm Structure Determined by Optical Coherence Tomography, *Nat. Sci. Rep.* 2019, 9, 9749.
35. Ohgaki, R., Teramura, Y., Hayashi, D., Quan, L., et al., Ratiometric fluorescence imaging on cell surface pH by poly(ethylene glycol)-phospholipid conjugated with fluorescein isothiocyanate, *Nat. Sci. Rep.* 2017, 7, 17484.
36. Adamberg, K., Kask, S., Laht, T. - M., Paalme, T., The effect of temperature and pH on the growth of lactic acid bacteria: a pH-auxostat study, *Int. J. Food Microbiol.* 2003, 85, 171–183.
37. Parente, E., Ricciardi, A., Addario, G., Influence of pH on growth and bacteriocin production by *Lactococcus lactis* subsp. *lactis* 140NWC during batch fermentation, *Appl. Microbiol. Biotechnol.* 1994, 41, 388–394.
38. Hofvendahl, K., van Niel, E. W. J., Hahn-Hägerdal, B., Effect of temperature and pH on growth and product formation of *Lactococcus lactis* ssp. *lactis* ATCC 19435 growing on maltose, *Appl. Microbiol. Biotechnol.* 1999, 51, 669–672.
39. Ohl, A. L., Wechselwirkungen von Stofftransport und Wachstum in Biofilmsystemen. Dissertation 2010. Paderborn: FIT-Verlag, Germany.
40. Vieira, M. J., Melo, L. F., Pinheiro, M. M., Formation B.: Hydrodynamic Effects on Internal Diffusion and Structure. *Biofouling* 1993, 7, 67–80.
41. Liu, Y., Shan, R., Chen, G., Liu, L., Linking flow velocity-regulated EPS production with early stage biofilm formation in drinking water distribution systems. *Water Supply* 2020, 20, 1253–1263.
42. Seker, S., Beyenal, H., Tanyolac, A., The effects of biofilm thickness on biofilm density and substrate consumption rate in a differential fluidized bed biofilm reactor (DFBBR). *J. Biotechnol.* 1995, 41, 39–47.
43. Cogan, N. G., Keener, J. P., The role of the biofilm matrix in structural development. *Math. Med. Biol.* 2004, 21, 147–166.
44. Melo, L. F., Biofilm physical structure, internal diffusivity and tortuosity. *Water Sci. & Technol.* 2000, 52, 77–84.
45. Zalc, J., Reyes, S. C., Iglesia, E., The effects of diffusion mechanism and void structure on transport rates and tortuosity factors in complex porous structures. *Chem. Eng. Sci.* 2004, 59, 2947–2960.
46. Guiot, E., Georges, P., Brun, A., Fontaine-Aupart, M. P., et al., Heterogeneity of diffusion inside microbial biofilms determined by fluorescence correlation spectroscopy under two-photon excitation. *Photochem. Photobiol.* 2002, 75, 570–578.
47. de Beer, D., Stoodley, P., Lewandowski, Z., Liquid flow and mass transport in heterogeneous biofilms. *Wat. Res.* 1996, 30, 2761–2765.

How to cite this article: Chodorski J, Hauth J, Strieth D, Wirsén A, Ulber R. Diffusion profiles in *L. lactis* biofilms under different conditions. *Eng Life Sci.* 2021;21:29–36.

<https://doi.org/10.1002/elsc.202000059>